

Fig. 1 State-of-the-art showing challenges in terms of in-line integration of continuous purification systems with flow platforms (a). Sketch for the integrated and continuous synthesis–purification process reported in this work, for the example of a Suzuki–Miyaura cross coupling reaction (b).

Significant efforts to integrate in-line purification by column chromatography with continuous-flow synthesis have been undertaken in recent years.⁹ The first method has been developed by Seeberger and co-workers, by coupling simulated moving-bed (SMB) chromatography with flow synthesis.^{9a} Here, a highly complex system has been used, consisting of a six-column configuration and 48-port valves. The use of multiple dual-mode centrifugal partition chromatography (MDM-CPC) has been also reported.^{9b} This kind of chromatography relies on the use of two non-miscible phases, instead of using a solid stationary phase. Selecting the two phases, or biphasic liquid system (BLS), is elaborate and time-consuming for benchtop application, as it needs to consider various operating parameters, such as the partition coefficients of product in the BLS and the settling time of the phases, which can determine the resolution of the separation. Two studies have been reported based on the use of multiple columns in parallel as a substitute of the countercurrent chromatography for the in-line purification. A supercritical fluid chromatography (SCFC) coupled with a multistep flow synthetic process has been reported by Ley and co-workers.^{9c} Despite the high overall yield of the process, this four-column system of 21 independent items of equipment with additional programming for automatic sampling require many specialists to operate. Vilela and co-workers investigated the use of in-line flash chromatography purification through a two-column configuration with a 10-port valve.^{9d}

All in-line purification technologies mentioned before provided significant advancements to this field, but their system complexity and low injection volumes per cycle (maximum 10 mL) clearly require further improvements. In

this work, we propose the capture-SMB technology as a new in-line purification approach, that offers high resolution, yield, and productivity, as well as low solvent consumption. This is achieved by utilizing only two twin columns and a new loading method, in which the product breaking through the outlet of a fully loaded first column is loaded onto the second column, thereby avoiding wasting precious material as well as increasing the process productivity. To integrate synthesis and purification, and build the end-to-end continuous process, a surge tank can be introduced to compensate the different flowrates of the synthesis and purification steps.¹⁰ As the mass transfer is improved between the liquid and the resin by the realization of a countercurrent movement between the stationary phase and the mobile phase, a higher resolution, or higher purity, is expected by the application of this technology. Moreover, a built-in software of the capture-SMB technology allows for fully automated operation and the minimum number of multi-port valves minimize the hold-up volume (Fig. 1b).

Experimental section

General information

All reactants were purchased from Sigma-Aldrich and used as such. Product characterization after reaction was done collecting an aliquot of the reaction product and analyzing it by high-performance liquid chromatography (HPLC). This was carried out on an Agilent 1100 series chromatograph equipped with a Thermo Scientific C18 Hypersil GOLD™ column (4.2 mL) and diode array detector (DAD) set at $\lambda = 210$ nm. In addition, ¹H and ¹³C nuclear magnetic resonance



(NMR) spectra of the products were recorded on a Bruker 400 MHz spectrometer. Batch reactions were performed using 20 mL round-bottom flasks. Flow reactions were conducted on a commercial Uniqsis™ flow microreactor, consisting of an HPLC pump, a T-shaped micromixer, a packed-bed reactor (diameter 1 cm, length 12 cm), a heating module, and a back-pressure regulator of 10 bar.

Synthesis of phenylboronic acid (2)

The synthesis of phenylboronic acid was performed either in a batch reactor or under continuous-flow conditions. For the batch experiments, to a stirred solution of bromobenzene **1** (1 mmol, 1 equiv.) in ethanol (5 mL, 0.2 M), dibenzylideneacetone palladium(0) phosphadmantane ethyl silica (1% mol) and KOAc (3 mmol, 3 equiv.) were added at room temperature. After stirring the mixture for 5 minutes, the heating was set to 80 °C, and the B₂(OH)₄ (1 mmol, 1 equiv.) was added. The mixture was kept under stirring for another 2 h. After this step, the mixture was cooled down to room temperature, and an aliquot of the reaction mixture was withdrawn for HPLC analysis. For the flow experiments, a solution of bromobenzene **1** (1 mmol, 1 equiv.), B₂(OH)₄ (1 mmol, 1 equiv.), and KOAc (3 mmol, 3 equiv.) in ethanol (5 mL) was pumped on the commercial Uniqsis™ flow microreactor. The solution passed through a column reactor, packed with dibenzylideneacetone palladium(0) phosphadmantane ethyl silica (1% mol), kept at fixed temperature. The product outlet was cooled down to room temperature, and an aliquot of the product mixture was withdrawn for HPLC analysis.

Synthesis of biphenyl (3)

The synthesis of biphenyl was performed either in a batch reactor or under continuous-flow conditions. For the batch experiments, dibenzylideneacetone palladium(0) phosphadmantane ethyl silica (1% mol) and KOAc (3 mmol, 3 equiv.) were added at room temperature to a solution of bromobenzene **1** (1 mmol, 1 equiv.) in ethanol (5 mL, 0.2 M). After stirring the mixture for 5 minutes, the heating was set to 150 °C, and phenylboronic acid **2** (1 mmol, 1 equiv.) was added to the reaction flask, and stirred for 1 h. After this step, the mixture was cooled down to room temperature, and an aliquot of the reaction mixture was withdrawn for HPLC analysis. For the flow experiments, a solution of bromobenzene **1** (1 mmol, 1 equiv.), phenylboronic acid **2** (1 mmol, 1 equiv.), and KOAc (3 mmol, 3 equiv.) in ethanol (5 mL) were pumped through a commercial Uniqsis™ flow microreactor. The solution passed through a column reactor, packed with dibenzylideneacetone palladium(0) phosphadmantane ethyl silica (1% mol), kept at fixed temperature. The product outlet was cooled down to room temperature, and an aliquot of the product mixture was withdrawn for HPLC analysis.

Synthesis of 1,3-bis[methyl(phenyl)amino]propan-2-ol (4)

A 2.8 M solution of epichlorohydrin (28 mmol, 1 equiv.) in EtOH and a 2.8 M solution of *N*-methylaniline (28 mmol, 1 equiv.) in EtOH were mixed and pumped through a stainless-steel coil reactor (internal volume = 60 mL) at 80 °C and 60 min. The product outlet was cooled down to room temperature, and an aliquot of the product mixture was withdrawn for HPLC analysis.

Synthesis of diphenyl ether (5)

Bromobenzene **1** (0.75 mmol, 1.5 equiv.), CuCl₂ (1% mol), and K₂CO₃ (1 mmol, 2 equiv.) were solubilized in a round-bottom flask using DMF (2 mL) as a solvent. The mixture was heated to 150 °C. At this temperature, phenol (0.5 mmol, 1 equiv.) was added. The mixture was kept under stirring for 24 h. After this step, the mixture was cooled down to room temperature, and an aliquot of the reaction mixture was withdrawn for HPLC analysis.

Purifications and capture-SMB technology

The purifications were conducted on a system comprising two long lifetime LED UV detectors (280 and 300 nm recorded simultaneously), and four high-precision double-piston pumps with active seal wash and one fraction collector. The system was equipped with two twin HPLC columns YMC-Triart Prep C18-S20 μm, each with a volume of 1.66 mL. The system was also supported by MControl, a dynamic software which keeps the process at the optimum. Breakthrough curves were collected using a solution composed by 25 mol% of phenylboronic acid and 75 mol% of biphenyl with a concentration of 3.5 mg mL⁻¹. Both batch chromatography and flow multi-column chromatography were performed using the same solution and a linear velocity of 300 cm h⁻¹.

The operating conditions of the capture-SMB technology were optimized using the results obtained from the breakthrough (BT) curves. As this twin-column technology uses an interconnected mode, in which the outlet of the upstream column is connected to the inlet of the downstream one, and a batch mode, in which the two columns are disconnected and operate in parallel, timings to switch from the batch to the interconnected mode and *vice versa* are essential in optimizing the operation of the technology. This process optimization can be easily achieved by inserting the BT points of the product (ranging from 1% to 10% of the product BT), and the desired loading volume (ranging from 65% to 85% of the product BT) obtained from the BT curves. These two experimental points determine the start and the end of the interconnected mode, respectively. After the first step of the process, in which the upstream column undergoes loading and the downstream column undergoes elution, cleaning and equilibration, the two columns are interconnected at the BT point defined for the process, which in this case is equal to 1%. Then, the two columns are disconnected when the desired BT of the



upstream column is reached, in this case equal to 70%. The upstream column undergoes the same phases of the downstream column in the first step (*i.e.*, elution, cleaning, and equilibration) while the downstream column continues the loading. In this way, using the twin-column technology efficiently loads the columns to maximize their resin utilization and thus allows for improving its productivity and solvent consumption.

Life cycle assessment

Given that the main reagent utilized (bromobenzene) is derived from fossil resources, the reduction of halobenzene usage would significantly improve the environmental performance of the product life cycle. In this sense, to evaluate the environmental profiles of the analyzed processes, we applied a life cycle assessment (LCA) methodology.¹¹ The LCA focused on the impacts associated with the production of the quantity of bromobenzene utilized per mg of final product. A cradle-to-gate scope and a cut-off system model based on mass allocation was defined. The environmental impact categories of global warming, fine particulate matter formation, and fossil resource scarcity were selected because, among the different 18 categories assessed in the ReCiPe midpoints impacts assessment method,¹² the impacts of bromobenzene production on these three categories contribute to over 90% of the aggregated environmental impacts on human health, ecosystems, and resources scarcity. Life cycle inventory for the production of bromobenzene was based on experimental data,^{12c} and the datasets for energy and materials flows based on European market from the life cycle inventory database (Ecoinvent 3.8).^{12d} The heating energy required in the bromobenzene preparation was thermodynamically estimated and adjusted by assuming an efficiency of 60% of the electric heating device.¹³ The stirring energy was calculated based on a required power of 3.2 W at 700 rpm for stirring a 10 g of mixture and extrapolated to the specific quantity in the bromobenzene experiment. Regarding facilities and transport, a chemicals plant of 50 000 ton yearly production with a 50 year lifespan and transport by lorry and train for distances of 100 km and 600 km were considered.¹⁴ Emissions to air during the process were assumed to be 0.2% of volatile input materials.^{14b} A 90% organic matter removal efficiency was assumed in the wastewater treatment, whose carbon is subsequently released into the air in the form of CO₂.^{14c} Finally, the impacts assessment results were obtained using the SimaPro 9.2 software.^{14d}

Circularity assessment

Different from the above LCA study, the circularity study investigated the formation of biphenyl, starting from three different halobenzene (chloro, bromo, and iodobenzene). The circularity methodology proposed by the Ellen MacArthur (EMA) foundation was applied, taking the material circular indicator (MCI) with values between 0

(linear) and 1 (circular).¹⁵ A production of 100 mg of pure biphenyl was assumed as functional unit. The processes considered were batch and continuous-flow synthesis and included the corresponding batch and continuous purification. To determine the impact of mass recycling, two scenarios were considered: (1) not considering reactant recycling and (2) considering reactant recycling. To this aim, the following hypotheses were taken: (i) all mass flows of the process were calculated according to the functional unit, so the material loads are different between process layouts, but the same between scenarios; (ii) the same reaction yields were taken for the different halogen-based derivatives; (iii) when a reactant was not recycled, it was considered as wasted; (iv) secondary wastes were not considered and, thus, the extraction efficiency (EF) of a recycled reactant was assumed as 100% in all cases; (v) the utility factor $F(X)$, which includes the product intensity and lifetime, was considered invariant in this study. All parameters used were defined according to the definitions and equations given by the Ellen MacArthur (EMA) foundation.¹⁵

Results and discussion

We initiated the work by optimizing the Suzuki–Miyaura reaction, a classical reaction applied in drug discovery and development, to prepare a biphenyl compound (Fig. 1b). The reaction is made of two steps: a Miyaura borylation where bromobenzene reacts with tetrahydroxydiboron to obtain phenylboronic acid, and a Suzuki C–C cross-coupling where the boronic acid obtained from the previous step reacts with bromobenzene to form biphenyl. The reactions were optimized on the commercial continuous-flow unit described before, equipped with a packed bed filled with Pd-based silica-supported heterogeneous catalyst (dibenzylideneacetone palladium(0) phosphadadamantane ethyl silica). Using a ‘design of experiments’ (DoE) approach, the borylation step was conducted in a systematic manner varying the temperature between 60 and 100 °C, and the residence time between 30 and 120 min. The two reactants were injected together, and the product yield was calculated by HPLC. The full experimental campaign is given in the ESI.† At the optimized 80 °C and 120 min conditions, the compound 2 was obtained with 86% yield (Fig. S1a†). To highlight the advantage of the continuous-flow synthesis, we performed at comparative experimental conditions (*i.e.*, 80 °C and 120 min) the same reaction in a standard round-bottom flask, obtaining compound 2 with only a 67% total yield under batch mode. As discussed elsewhere, the higher yield in flow conditions can be ascribed to the improved contact of the liquid phase with the catalytic sites in flow.¹⁶ The second step was performed by using the same continuous set-up described above. The formation of biphenyl was performed by injecting an ethanolic solution of bromobenzene and phenylboronic acid in the packed-bed reactor. Following the DoE approach, the reaction was conducted at different



temperatures (from 100 to 150 °C) and residence times (from 30 to 120 min). The maximum yield of compound 3 (58%) was achieved at 150 °C and 60 min (Fig. S1b†). Under batch conditions, compound 3 was achieved with only 45% yield, thus testifying the improvement brought by flow conditions.

Having optimized the synthesis, we integrated the two continuous steps together to prepare biphenyl in one pot. We then moved to the development of a suitable purification process. We started from the traditional batch chromatography, in which the crude mixture is discontinuously loaded into a column, packed with a C18

resin, until its capacity is approached. The biphenyl compound obtained from the Suzuki–Miyaura reaction served as model species to demonstrate the effectiveness of this multidisciplinary approach. A breakthrough test was preliminarily carried out on the reaction product in order to determine the dynamic binding capacity of the resin, which is pivotal for establishing the conditions for its optimal utilization (Fig. 2a). The crude, at 2.37 mg mL⁻¹ of product 3, was loaded onto 1.66 mL of C18 resin and the product concentration in the eluate of the column was measured through a calibrated in-line UV-vis detector. The 1%

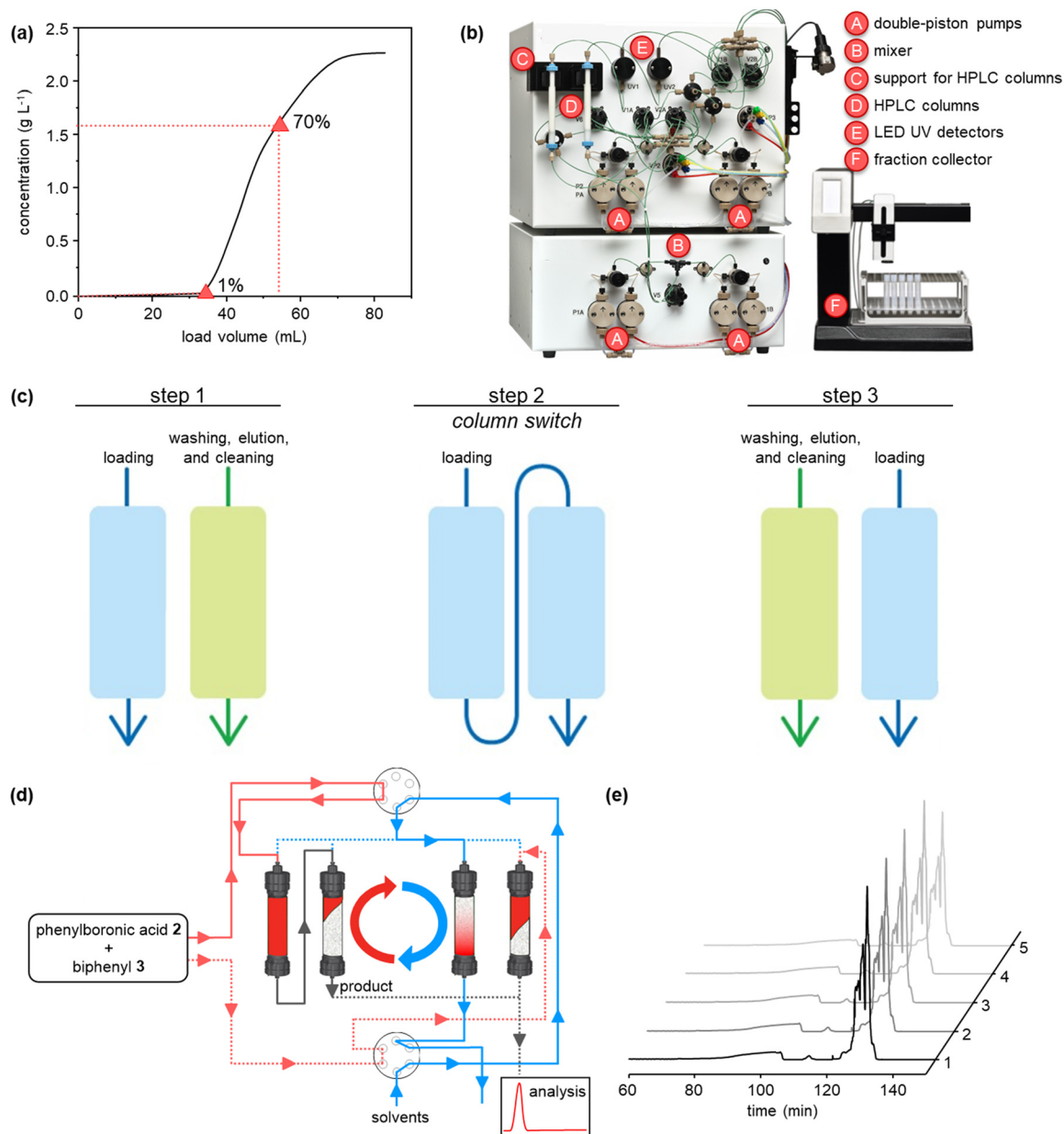


Fig. 2 Breakthrough curve for biphenyl product during batch and continuous chromatographic purification (a), showing improved performance over a multi-column continuous setup; photograph of the modified continuous moving bed chromatography setup (b); schematic representation of a half-cycle of the continuous operation, for the loading, washing, elution, and cleaning steps (c); schematic flow diagram of the continuous chromatography setup (d); UV traces of the five performed cycles during continuous synthesis and product purification (e).



Table 1 Comparison between batch and continuous-flow purification processes in the purification of biphenyl

	Solvent consumption (L g ⁻¹)	Isolated yield (%)	Productivity (g h ⁻¹ L ⁻¹)	Purity (%)
Batch ^a	1.4	51.3	17.2	86.3
Continuous-flow ^a	0.3	81.3	22.7	>99
Process gain ^b (batch vs. continuous-flow)	79.6%	58.5%	31.6%	15.9%

^a Synthesis and purification conditions in Fig. 1b and in the ESI.† ^b Process improvement between continuous-flow and batch experiments.

breakthrough (BT), *i.e.*, 1% of the product concentration in the feed, was measured in the eluate after having loaded 34 mL of crude. Considering the operating linear velocity of 300 cm h⁻¹, the saturation time corresponding to the 1% BT was 61.5 min.¹⁷ This means that, reached this loading volume, the product starts being lost in the eluate, with no more adsorption on the resin, compromising the yield of the process. This was then considered as the reference loading for a batch single-column chromatography in order to avoid sacrificing the yield of the product. In this condition, a resin loading of 48.5 mg mL_{resin}⁻¹ was achieved. Using this parameter, the initial separations were performed in batch. The crude, with an overall concentration of 3.5 mg mL⁻¹, was loaded up to the 1% BT estimated previously. After the loading, a washing step with 14 mM Na₂CO₃ was performed to desorb the impurities. Finally, the elution was operated with a step gradient to 100% acetonitrile and 1 mL fractions were collected during this phase to characterize the process. In particular, the yield and the biphenyl concentration in each fraction were determined by at-line HPLC analysis. The overall purity of the biphenyl collected from the batch process was about 86%. The yield, defined as the ratio between collected and injected product, was 51% for the batch process, while the productivity is 17 g h⁻¹ L_{resin}⁻¹ (Table 1). This poor yield was ascribed to the breakthrough of some product in the loading phase as well as in the washing step, required to desorb the impurities and reach acceptable standards of purity.

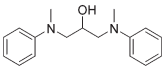
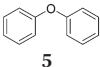
In order to improve the downstream processing performances, we moved to a continuous countercurrent chromatography process based on two twin columns, directly applying it to our small molecules.¹² In this approach, the crude is partialized into multiple columns, which undergo consecutive interconnected (series) and disconnected (parallel) operations ensuring the periodic continuity of the

feeding and the necessary steps of cleaning-in-place and regeneration. This leads to higher resin utilization and process efficiency, due to the maximized driving force for mass transfer, ensured by the simulated countercurrent movement between the solid and liquid phases, and therefore an easier scalability for industrial processes. The set-up was composed by two supports for columns, two long lifetime LED UV detectors (280 and 300 nm recorded simultaneously), four high precision double-piston-pumps with active seal wash and one pump for feed supply. The chromatograph was equipped with two HPLC columns YMC-Triart Prep C18-S20 μm, each with a volume of 1.66 mL (Fig. 2b).

The purification cycle involved two phases (Fig. 2c and d): in the first one, the columns are interconnected and are employed in series to ensure that the product breaking through the upstream column during the loading is re-adsorbed in the downstream one. This allowed to push the loading phase to higher values of breakthrough. In this work, 70% BT, corresponding to a loaded volume of 54 mL, was applied. This enabled a higher loading of the resin, up to 77 mg mL_{resin}⁻¹, which in turns grants a better column utilization compared to the single-column configuration. In the second stage, the columns are employed in parallel, performing the washing, elution and regeneration of the upstream column while completing the loading of the downstream one. These two phases constitute a switch, after which the two columns reach the same initial conditions but with exchanged positions (*i.e.*, the upstream column becomes the downstream one and *vice versa*). Then, a full cycle comprises two symmetrical switches.

In our work, with only five cycles, we were able to purify the compounds. The UV traces recorded at the outlet of one of the two columns for these five cycles are shown in Fig. 2e,

Table 2 Continuous synthesis of other small molecules^a

	Solvent consumption (L g ⁻¹)	Isolated yield (%)	Productivity (g h ⁻¹ L ⁻¹)	Purity (%)
	2.4	68	7.5	93
	2.4	71	7.1	92

^a Synthesis and purification conditions in the ESI,† Tables S1 and S2.



on fossil resources scarcity are halved by switching the production process from batch to flow systems. A similar positive outcome was determined for the environmental impact categories fine particulate matter formation and fossil resource scarcity. Together with the global warming, this provides a forecast both for most urgent global issues (warming, resources) and human health (particulate matter).

The circularity assessment goes one step further in scope than the LCA, by considering the route to generate biphenyl. As the focus is on recycling, the lost and recovered mass loads determine the degree of circularity. The mass loads are reduced when switching from batch to continuous-flow, both for the synthesis and purification (Table 3).¹⁸ In this sequence, the demand of virgin materials (V) decreases when the process is carried out continuously. Additionally, the recycled fraction (FR) is increased to a maximum value of 0.81, for a continuous synthesis and purification with reactants recycled and assuming synthesis using chlorobenzenes (Table S3†). Waste generation is also positively impacted, reaching a 95% reduction when using chloro-benzenes. The MCI metrics scores largest (0.859) for the best scenario. To summarise, the two-fold continuous process, continuous in synthesis and purification, is considerably better in the environmental performance, as evidenced by the LCA study. The circularity study confirmed this outcome, and outlined that the results would be significantly better when considering recycling of reactant waste and replacing the bromohalogens of the study with chlorohalogens.

Conclusions

In conclusion, we have presented an improved protocol for the end-to-end synthesis and multi-column preparative purification of small molecules, in an integrated manner and under continuous conditions. The approach was demonstrated for the synthesis of structurally-different organic compounds. In all cases, the flow method demonstrated higher product yields, quick product isolation, and reduced solvent consumption compared to traditional batch-type chromatography. Circularity and life cycle analyses further highlighted the environmental benefits for the integrated flow process. The approach may find applications in the design of new synthesis–purification–analysis platforms applied in drug discovery.

Author contributions

AS, VR, and RL synthesized and characterized the small molecules, optimizing batch and flow protocols. TKK and AS performed the chromatographical purifications in batch and continuous conditions. JO-T, ME-G, and VH performed the circularity and environmental analyses. GV contributed for funding acquisition. GV and MS supervised the research work. AS, TKK, MS, and GV wrote the manuscript with

contributions and discussions from all authors. All authors have given approval to the final version of the manuscript.

Conflicts of interest

There are no conflicts to declare.

Acknowledgements

Funding from the European Commission (GV, grant agreement 101031710), Bracco Imaging (AS, VR, and GV), Fondazione Bracco (GV), and YMC Japan (TKK and MS) is gratefully acknowledged. The authors thank Maria Suanno and Martina Villa for collecting experimental data on Suzuki coupling. Professor Massimo Morbidelli is thanked for useful discussions on continuous manufacturing.

Notes and references

- (a) Y. Mo, G. Rughoobur, A. M. K. Nambiar, K. Zhang and K. F. Jensen, *Angew. Chem., Int. Ed.*, 2020, **59**, 20890; (b) S. V. Ley, *Angew. Chem., Int. Ed.*, 2018, **57**, 5182.
- (a) T. Wan, L. Capaldo, G. Laudadio, A. V. Nyuchev, J. A. Rincón, P. García-Losada, C. Mateos, M. O. Frederick, M. Nuño and T. Noël, *Angew. Chem., Int. Ed.*, 2021, **60**, 17893; (b) P. Musci, T. von Keutz, F. Belaj, L. Degennaro, D. Cantillo, C. O. Kappe and R. Luisi, *Angew. Chem., Int. Ed.*, 2021, **60**, 6395.
- (a) K. Lovato, P. S. Fier and K. M. Maloney, *Nat. Rev. Chem.*, 2021, **5**, 546; (b) R. C. R. Wootton and A. J. deMello, *Nature*, 2012, **483**, 43.
- (a) A. M. Schweidtmann, A. D. Clayton, N. Holmes, E. Bradford, R. A. Bourne and A. A. Lapkin, *Chem. Eng. J.*, 2018, **352**, 277; (b) S. M. Kearnes, M. R. Maser, M. Wleklinski, A. Kast, A. G. Doyle, S. D. Dreher, J. M. Hawkins, K. F. Jensen and C. W. Coley, *J. Am. Chem. Soc.*, 2021, **143**, 18820; (c) P. Sagmeister, R. Lebl, I. Castillo, J. Rehr, J. Kruisz, M. Sipek, M. Horn, S. Sacher, D. Cantillo, J. D. Williams and C. O. Kappe, *Angew. Chem., Int. Ed.*, 2021, **60**, 8139; (d) I. W. Davies, *Nature*, 2019, **570**, 175.
- (a) A. Sivo, V. Ruta and G. Vilé, *J. Org. Chem.*, 2021, **86**, 14113; (b) S. Tortoioli, A. Friedli, A. Prud'homme, S. Richard-Bildstein, P. Kohler, S. Abele and G. Vilé, *Green Chem.*, 2020, **22**, 3748.
- (a) A. Adamo, R. L. Beingessner, M. Behnam, J. Chen, T. F. Jamison, K. F. Jensen, J.-C. M. Monbaliu, A. S. Myerson, E. M. Revalor, D. R. Snead, T. Stelzer, N. Weeranoppanant, S. Y. Wong and P. Zhang, *Science*, 2016, **352**, 61; (b) A. Gioiello, A. Piccinno, A. M. Lozza and B. Cerra, *J. Med. Chem.*, 2020, **63**, 6624.
- (a) J. Imbrogno, L. Rogers, D. A. Thomas and K. F. Jensen, *Chem. Commun.*, 2018, **54**, 70; (b) N. Weeranoppanant and A. Adamo, *ACS Med. Chem. Lett.*, 2020, **11**, 9; (c) I. V. Gürsel, N. Kockmann and V. Hessel, *Chem. Eng. Sci.*, 2017, **169**, 3.
- (a) B. J. Doyle, P. Elsner, B. Gutmann, O. Hannaerts, C. Aellig, A. Macchi and D. M. Roberge, *Org. Process Res. Dev.*, 2020, **24**, 2169; (b) K. Wen, C. Hu, W. Wu, K. Shvedova, S. C.



- Born, B. Takizawa and S. Mascia, *Org. Process Res. Dev.*, 2021, **25**, 1853.
- 9 (a) A. G. O'Brien, Z. Horváth, F. Lévesque, J. W. Lee, A. Seidel-Morgenstern and P. H. Seeberger, *Angew. Chem., Int. Ed.*, 2012, **51**, 7028; (b) R. Örkényi, J. Éles, F. Faigl, P. Vincze, A. Prechl, Z. Szakács, J. Kóti and I. Greiner, *Angew. Chem., Int. Ed.*, 2017, **56**, 8742; (c) D. E. Fitzpatrick, R. J. Mutton and S. V. Ley, *React. Chem. Eng.*, 2018, **3**, 799; (d) C. G. Thomson, C. Banks, M. Allen, G. Barker, C. R. Coxon, A. L. Lee and F. Vilela, *J. Org. Chem.*, 2021, **86**, 14079.
- 10 (a) D. J. Karst, F. Steinebach and M. Morbidelli, *Curr. Opin. Biotechnol.*, 2018, **53**, 76; (b) S. Vogg, T. Müller-Spáth and M. Morbidelli, *Curr. Opin. Chem. Eng.*, 2018, **22**, 138; (c) V. Warikoo, R. Godawat, K. Brower, S. Jain, D. Cummings, E. Simons, T. Johnson, J. Walther, M. Yu, B. Wright, J. McLarty, K. P. Karey, C. Hwang, W. Zhou, F. Riske and K. Konstantinov, *Biotechnol. Bioeng.*, 2012, **109**, 3018; (d) R. Godawat, K. Konstantinov, M. Rohani and V. Warikoo, *J. Biotechnol.*, 2015, **213**, 13; (e) F. Feidl, S. Vogg, M. Wolf, M. Podobnik, C. Ruggeri, N. Ulmer, R. Wälchli, J. Souquet, H. Broly, A. Butté and M. Morbidelli, *Biotechnol. Bioeng.*, 2020, **117**, 1367.
- 11 *Environmental management — Life cycle assessment — Principles and framework*, <https://www.iso.org/standard/37456.html>, 2006.
- 12 (a) ReCiPe 2016 v1.1 endpoint method, Hierarchist version; (b) M. A. J. Huijbregts, Z. J. N. Steinmann, P. M. F. Elshout, G. Stam, F. Veronesi, M. D. M. Vieira, A. Hollander, M. Zijp and R. van Zelm, *Int. J. Life Cycle Assess.*, 2017, **22**, 138–147; (c) B. S. Furniss, A. J. Hannaford, P. W. G. Smith and A. R. Tatchell, *Vogel's textbook of practical organic chemistry*, Longman Scientific & Technical, London, 5th edn, 1989, vol. 143; (d) Ecoinvent LCA database, <https://ecoinvent.org/>, 2022.
- 13 J. Osorio-Tejada, F. Ferlin, L. Vaccaro and V. Hessel, *Green Chem.*, 2022, **24**, 325–337.
- 14 (a) R. Frischknecht, N. Jungbluth, H.-J. Althaus, G. Doka, R. Dones, S. Hellweg, R. Hischier, T. Nemecek, G. Rebitzer and M. Spielmann, *Int. J. Life Cycle Assess.*, 2005, **10**, 112–122; (b) R. Hischier, S. Hellweg, C. Capello and A. Primas, *Int. J. Life Cycle Assess.*, 2005, **10**, 59–67; (c) H.-J. Althaus, M. Chudacoff, R. Hischier, N. Jungbluth, M. Osses and A. Primas, *Ecoinvent report No. 8*, 2007, v2.0; (d) PRé Consultants, <https://pre-sustainability.com/solutions/tools/simapro/>, 2022.
- 15 The Ellen MacArthur Foundation Circularity Indicators, <https://ellenmacarthurfoundation.org/resources/circulytics/overview> (Accessed August 2022).
- 16 (a) A. Simoens, T. Scattolin, T. Cauwenbergh, G. Pisanò, C. S. J. Cazin, C. V. Stevens and S. P. Nolan, *Chem. – Eur. J.*, 2021, **27**, 5653; (b) S. Govaerts, A. Nyuchev and T. Noël, *J. Flow Chem.*, 2020, **10**, 13–71; (c) T. Noël and S. L. Buchwald, *Chem. Soc. Rev.*, 2011, **40**, 5010–5029.
- 17 (a) E. Shahbazali, E. M. F. Billaud, A. S. Fard, J. Meuldijk, G. Bormans, T. Noël and V. Hessel, *AIChE J.*, 2020, **67**, e17067; (b) M. Angarita, T. Müller-Spáth, D. Baur, R. Lievrouw, G. Lissens and M. Morbidelli, *J. Chromatogr. A*, 2015, **1389**, 85; (c) T. K. Kim, C. Botti, J. Angelo, X. Xu, S. Ghose, Z. J. Li, M. Morbidelli and M. Sponchioni, *Ind. Eng. Chem. Res.*, 2021, **60**, 10764.
- 18 M. Escribà-Gelonch, G. A. de Leon Izeppi, D. Kirschneck and V. Hessel, *ACS Sustainable Chem. Eng.*, 2019, **7**, 17237–17251.

